RADIATION AND POWER DEPOSITION STUDIES FOR THE FCC-ee HALO COLLIMATION SYSTEM

S. Marin*, G. Banks, G. Broggi, R. Bruce, R. Cowan, A. Frasca, B. Humann,
A. Lechner, G. Lerner, G. Nigrelli, A. Perillo Marcone, K. Taylor
European Organization for Nuclear Research (CERN), Geneva, Switzerland

Abstract

The collimation system of the Future Circular Collider (FCC-ee) is essential to isolate losses away from the experiments and other machine elements, thus reducing the radiation background in the experiments, and avoiding damage to the machine in case of accidental beam losses. The primary and secondary collimators of the collimation hierarchy, employed to scatter halo particles from the beam and remove them, respectively, will be accommodated in one of the technical insertions of the collider ring (Point F). In this paper, FLUKA simulations are presented for the collimation straight section. The power deposition is determined for all elements in the section following beam impacts on the collimator jaws, including other collimators as well as dipole and quadrupole magnets. Finally, the paper discusses the radiation levels in the Point F tunnel resulting from beam losses on the collimation system, and the resulting radiation hardness requirements for machine equipment and infrastructure.

INTRODUCTION

The FCC-ee collimation system [1–3] is designed to protect machine equipment and detectors from beam losses and to reduce the experimental background in the 91 km electron-positron collider [4]. In a previous study [5], we assessed the power deposition induced by beam halo losses in the collimation insertion, using FLUKA Monte Carlo simulations [6–9]. That work demonstrated that, for the GHC (Global Hybrid Correction) optics v23 considered at the time, two strategically placed shower absorbers can intercept secondary radiation between primary and secondary collimators, reducing the power leaking to the environment from approximately 50 % to 15 % of the total halo-loss power.

This paper extends our earlier study in several directions. First, we present results for the LCC (Local Chromaticity Correction) optics v105 with a two-phase betatron collimation layout, now featuring four primary and six secondary collimators distributed over approximately 2 km of the straight section at Point F. Second, we investigate the radiation environment in the tunnel, quantifying the absorbed dose and equivalent particle fluences relevant for the radiation hardness requirement of machine equipment. Third, we briefly assess the contribution of synchrotron radiation to the overall radiation levels in the collimation insertion, comparing the photon spectra in Z-pole and $t\bar{t}$ operation modes.

* stefano.marin@cern.ch

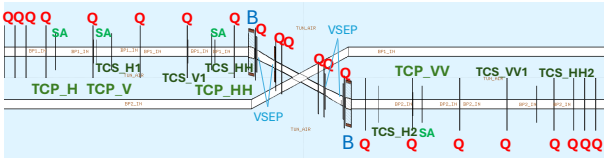

Figure 1: FLUKA geometry model of the betatron cleaning system including primary and secondary collimators, showing the location of optical and collimation system elements.

COLLIMATION SYSTEM AND SIMULATION MODEL

The simulation is performed with the FLUKA Monte Carlo code. The geometry model comprises a concrete tunnel of 5.5 m inner-bore diameter housing two 6 cm diameter copper vacuum chambers separated by 35 cm. The primary collimators (TCP) consist of a 25 cm-long graphite absorber with a TZM frame, while the secondary collimators (TCS) use a 30 cm-long TZM absorber. Both designs feature a double tapered jaw geometry at 9.5° on both upstream and downstream, with space to accommodate a beam position monitor. The jaws, including the tapers, measure 67 cm and 72 cm for primary and secondary collimators, respectively.

The full geometry of Point F is shown in Fig. 1, which illustrates the location of the magnets (Q for quadrupoles, B for bending, VSEP for vertical separators) and collimators (TCP for primary, TCS for secondary), as well as preliminary shower absorbers (SA), placed downstream of primary collimators to intercept radiation showers before they interact with the machine. Table 1 lists the half-gaps and positions for all collimators on the positron beamline. The two-phase collimation system features two primary collimators for each orientation, followed by secondary collimators. Due to limited space, only one secondary collimator for vertical betatron cleaning can be accommodated. We note that the LCC optics decouple the betatron and momentum collimation system, and Point-F will be dedicated to the former.

Table 1: Collimator Half-Gaps Δ and Positions s

	Δ (mm)	s (m)		Δ (mm)	s (m)
TCP.H	5.707	146.3	TCS.HH1	2.451	817.0
TCP.V	2.066	302.6	TCS.H2	5.023	1249.6
TCS.H1	4.999	362.8	TCP.VV	2.070	1364.3
TCS.V1	2.494	616.1	TCS.VV1	2.407	1677.8
TCP.HH	3.744	695.6	TCS.HH2	5.694	1775.5

The expected halo-loss power, listed in Table 2, is the source term considered in the FLUKA simulations of this

work. Beam halo losses give rise to high-energy electromagnetic showers, which require the multi-stage collimation system described here. The nominal beam lifetime, shared in principle between momentum and betatron losses but assumed here to be only of betatron character, is 20 min. It is also expected that the lifetime could drop to 5 min, although this would only have to be sustained for a few seconds. As source term for beam halo losses in the FLUKA model, we simulate a positron pencil beam impacting the midpoint of the primary collimator jaws, with an impact parameter of 1 µm relative to the jaw edge. Impacts are evenly sampled on the jaws of each of the primary collimators.

Table 2: Radiation Sources and Emitted Power in the Collimation Insertion (PF), per Beam

Type	Z-pole		$t\bar{t}$
	Avg. power	Lifetime drop	Avg. power
Betatron halo	14.6 kW	58.8 kW	0.45 kW

ENERGY DEPOSITION

Due to the large amount of radiation leaking to machine elements and the tunnel environment, we have preliminarily investigated the use of shower absorbers in the collimation section. A similar study was carried out for the GHC optics in our earlier work [5]; the work present here is more complex, with four primary collimators instead of two, and a full optimization process has not been completed yet. For the preliminary configuration of shower absorbers, we compare in Table 3 the power absorbed in different machine elements in Point F, grouped by function. The summed power is given both in relative and absolute terms; the absolute values are scaled to a 5 min lifetime. The "Environment" column in the table shows the power delivered to the vacuum pipe, the tunnel, and the surrounding earth. It is expected that with a better optimization of the absorber locations, the power dissipated in the environment will be reduced further.

One of the design constraints of the collimation system is that it must be able to sustain the power delivered by beam losses during normal operation, lifetime drops, as well as certain accidental scenarios. During normal halo loss scenarios, the most loaded collimators are the secondaries (and shower absorbers, if present), which are impacted by the high-energy electromagnetic showers propagating from the primary. It is important that in the envisaged scenarios, these collimators are robust enough to sustain the resulting power load without being damaged. In Fig. 2, we show the power absorption map for the most impacted collimator element, TCS_H1 in the case of a lifetime drop, averaged over ±1 mm in the direction transverse to the beam. The level of power density, at most 100 W/cm^3 is acceptable. Furthermore, the total power absorbed by any collimator jaw, in the case of a lifetime drop, is limited to 4 kW, in the shower absorber or collimator jaws, below the predicted level of power absorption in HL-LHC, ≈ 10 kW.

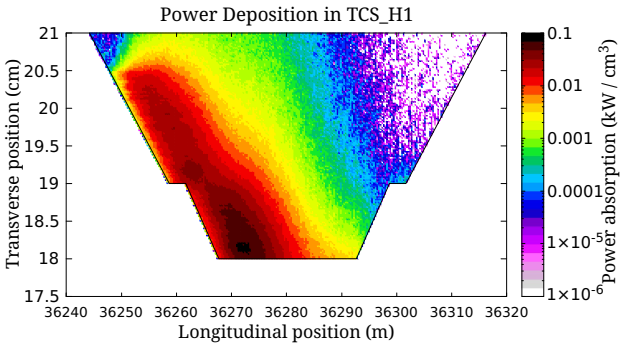

Figure 2: Power deposition map of secondary collimator TCS_H1 during lifetime drop losses.

Finally, we discuss the accidental scenario of full beam bunches impacting directly on a primary collimator, a scenario which may materialize as a consequence of beam instabilities. Following recent findings [10], we assume that graphite can sustain at least 5 kJ/g, which translates to approximately 40 bunches, if these impact centrally on the face of the collimator, with a large impact parameter (5 σ clearing from the edge).

RADIATION LEVELS IN THE TUNNEL

Maintaining manageable radiation levels in the tunnel is essential for the lifetime of radiation-sensitive equipment like cables, optical fibres and electronics. As shown in Table 2, the Z-mode halo losses produce a much higher power deposition than in the $t\bar{t}$ mode, since the beam intensity scales inversely with the fourth power of the beam energy. Figure 3 presents the key quantities relevant for cumulative radiation damage in materials and electronics (absorbed dose and 1 MeV neutron equivalent fluence on silicon) as well as for single event effects in electronics (high-energy hadron equivalent fluence and thermal neutron equivalent fluence). All scored quantities shown in Fig. 3 are averaged over ±20 cm around the beam plane in vertical direction. The dose levels can reach the MGy/yr range in the vicinity of the collimators, indicating that radiation-hard equipment will be required in the collimation straight section. A dedicated strategy for electronics needs to be developed, for example by housing electronics in shielded areas or in distant alcoves.

In addition to the radiation fields generated by halo-induced electromagnetic showers, the collimation insertion also receives a contribution from synchrotron radiation. The total SR power, 109 kW per beam in all operation modes, exceeds the halo-loss power. In Z mode operation, where halo losses are strongest, the much softer photon spectrum makes it considerably easier to shield. Figure 4 compares the photon spectra in the Z and $t\bar{t}$ modes: while the total emitted power is identical by design, the spectral characteristics differ significantly. In Z-mode the photon energies are limited to a few keV (critical energy $E_c \approx 20$ keV), and are readily absorbed within the vacuum chamber and surrounding dipole structures. In $t\bar{t}$-mode, however, the much harder spectrum ($E_c \approx 1.2$ MeV) is sufficiently high to trig-

Table 3: Energy Absorption With and Without Shower Absorbers

	Primary collimators		Shower absorbers		Secondary collimators		Magnets		Environment	
	kW	% of total	kW	% of total	kW	% of total	kW	% of total	kW	% of total
Without absorbers	0.47	0.80	—	—	23.90	40.80	0.57	0.98	33.63	57.41
With absorbers	0.24	0.41	21.11	36.00	17.76	30.29	0.26	0.44	19.27	32.86
Change (%)	−48.60	—	—	—	−25.69	—	−55.12	—	−42.69	—

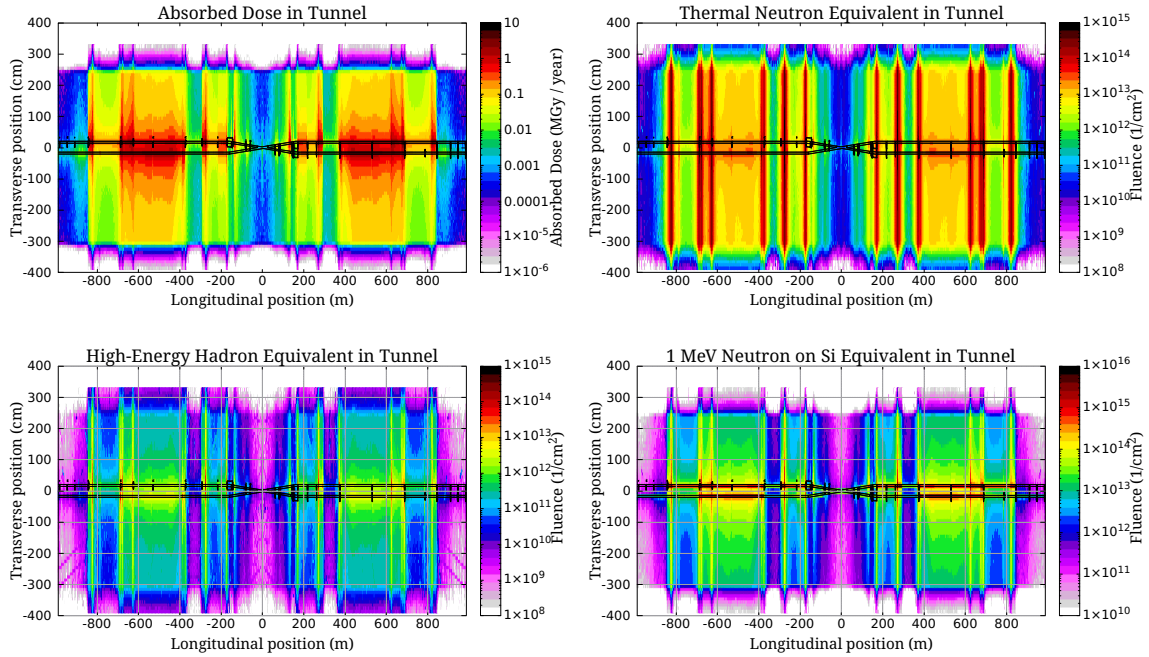

Figure 3: FLUKA simulation of radiation levels in the tunnel of the betatron collimation section: absorbed dose, high-energy hadron equivalent fluence, 1 MeV neutron equivalent fluence on silicon, and thermal neutron equivalent fluence.

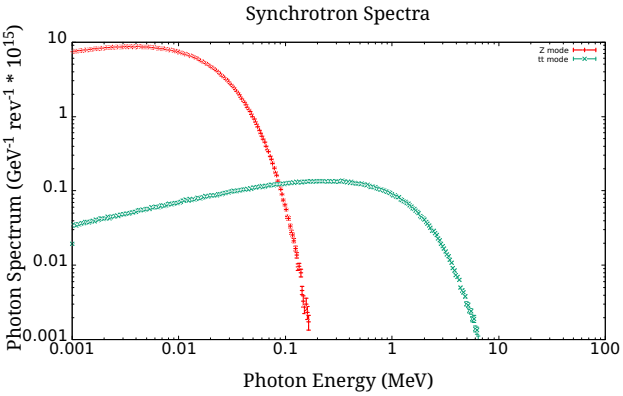

Figure 4: Photon spectra emitted as synchrotron radiation during the bending of the beam in the collimation section, per revolution and per beam.

ger photo-nuclear reactions, and can significantly elevate the dose levels in the surrounding environment. Dedicated shielding studies for this scenario will be performed in future work.

CONCLUSION

We have presented FLUKA Monte Carlo simulations of the radiation and power deposition in the FCC-ee betatron collimation section, extending our earlier work [5] with an updated collimation layout and new studies of the radiation environment. Radiation levels in the tunnel can reach the MGy/yr scale in the Z-mode, imposing stringent radiation hardness requirements on equipment in the collimation insertion. While synchrotron radiation dominates the total power loss, its impact on radiation levels is mode-dependent, with the harder photon spectrum in $t\bar{t}$ operation posing additional shielding challenges that will be addressed in future studies.

REFERENCES

[1] M. Hofer *et al.*, "Design of a Collimation Section for the FCC-ee", in *Proc. IPAC'22*, Bangkok, Thailand, Jun. 2022, pp. 1722–1725. doi:10.18429/JACoW-IPAC2022-WEPOST017

[2] G. Broggi, A. Abramov, and R. Bruce, "Beam dynamics studies for the FCC-ee collimation system design", in *Proc. IPAC'23*, Venice, Italy, May 2023, pp. 360–363. doi:10.18429/JACoW-IPAC2023-MOPA129

[3] G. Broggi *et al.*, "Optimizations and updates of the FCC-ee collimation system design", in *Proc. IPAC'24*, Nashville, TN, May 2024, pp. 2673–2676. doi:10.18429/JACoW-IPAC2024-TUPC76

[4] A. Abada *et al.*, "FCC-ee: The Lepton Collider", *Eur. Phys. J. Spec. Top.*, vol. 228, pp. 261–623, Jun. 2019. doi:10.1140/epjst/e2019-900045-4

[5] S. Marin *et al.*, "Power deposition studies for the FCC-ee halo collimation system", in *Proc. IPAC'25*, Taipei, Taiwan, Jun. 2025, pp. 486–489. doi:10.18429/JACoW-IPAC2025-MOPM069

[6] FLUKA Official Website, `https://fluka.cern`

[7] C. Ahdida *et al.*, "New Capabilities of the FLUKA Multi-Purpose Code", *Frontiers in Physics*, vol. 9, p. 788253, Jan. 2022. doi:10.3389/fphy.2021.788253

[8] G. Battistoni *et al.*, "Overview of the FLUKA code", *Annals of Nuclear Energy*, vol. 82, pp. 10–18, 2015. doi:10.1016/j.anucene.2014.11.007

[9] V. Vlachoudis, "FLAIR: A powerful but user friendly graphical interface for FLUKA", in *Proc.M&C 2009*, Saratoga Springs, NY, USA, May 2009.

[10] A. L. Lund *et al.*, "Towards the detailed design of the High Luminosity Large Hardon Collider Beam dumps", presented at the IPAC'26, Deauville, France, May 2026, paper THP4110, this conference.